Progress In Electromagnetics Research B, Vol. 40, 141–158, 2012

RIGHT-ANGLED TRIANGULAR PATCH RESONATOR AND FILTER WITH FRACTAL HOLE

J.-K. Xiao[1, 2, *], X.-P. Zu[3], X. Li[3], and L. Tian[3]

[1]School of Electronical & mechanical Engineering, Xidian University, Xi'an 710071, China

[2]State Key Laboratory of Millimeter Waves, Nanjing 210096, China

[3]School of Computer and Information, Hohai University, Changzhou 213022, China

Abstract—Fractal-shaped microwave passive circuits offer a great deal of promise for achieving good performance in small circuits. In this paper, isosceles right-angled triangular patch resonator with fractal hole is analyzed, and new single-band and dual-band RF filters by using isosceles right-angled triangular patch resonators with fractal pattern are proposed. It is shown that the right-angled triangular resonator can be miniaturized with the assistance of a fractal, and filter performance is greatly improved. Simultaneously, the resonator's higher order mode resonance is fortified, easing off the difficulty in dual-band filter design. Two proposed fractal bandpass filters are fabricated, and their performance is verified by measurement. The proposed filters demonstrate the applications of right-angled triangular patch resonator and exhibit advantages of a simple structural topology and compactness, which are essential in RF circuit design.

1. INTRODUCTION

Triangular patch resonators [1–6], especially the equilateral triangular resonator and isosceles right-angled triangular (IRT) resonator, have important applications in microwave circuits with existing design methods. However, the IRT resonator received less attention. The good performance of triangular patch filters have been proven; however, few works have been reported compared with the square

Received 6 February 2012, Accepted 6 April 2012, Scheduled 16 April 2012

* Corresponding author: Jian-Kang Xiao (xiaojk@lzu.edu.cn).

and circular patch filters [4]. In [1, 3], bandpass and bandstop filters are developed by using equilateral triangular resonators, and in [2], new wide band bandpass filter using multi-mode equilateral triangular resonator is designed. [5] develops new isosceles triangular resonator for a wide-band bandpass filter, and [6] reports novel bandpass filters with controllable operation by using equilateral triangular resonator. However, these works only possess one single operation band, and multi-band is not concerned. Compared with the transmission-line based filters, patch filters have more compact size, lower loss, and higher power handling features. The basic principle for designing a patch resonator filter is the selectivity and usage of all sorts of resonant modes. In the past, patch filter design mainly concentrates on dual-mode (the dominant mode and its degenerate one) operation, and the higher order modes are not considered.

Nowadays, fractal technique [2, 7–10] attracts great attention of microwave researchers in designing new microwave circuits and improving circuit's performance. However, their works focus on antennas, not on filters. Fractal has inherent properties, which are self-similarity and space filling. The typical fractals with their shape and dimensions decided by certain mathematic method always are strictly self-similar, and can be called well-regulated or regular fractals. Those not-carefully-designed fractal configurations applied in RF circuit, however, are irregular fractals with rough self-similarity. In RF circuits design, fractal can be used in building patch resonators, microstrip lines, and the defected ground of microstrip. Fractal has the advantages of miniaturization, wide bandwidth, and multi-band operation in the filters design. Fractal hole in a patch provides the latter with a field perturbation and introduces higher order modes for multi-band operation. It also realizes circuit miniaturization and wide-band performance.

In this paper, a fractal-shaped IRT resonator is proposed, and novel RF filters with single- and dual-band using IRT resonator are designed with the usage of a fractal, which acts as a field perturbation, resulting in desired higher order mode. The obtained higher order mode is utilized to implement the filter's dual-band response. The fractal not only miniaturizes circuit size but also greatly improves filter performance.

2. ISOSCELES RIGHT-ANGLED TRIANGULAR PATCH RESONATOR

Resonant frequency of the isosceles right-angled triangular patch resonator can be expressed as [11]

$$f_r = \frac{c}{2L\sqrt{\varepsilon_r}}\sqrt{m^2 + mn + 2n^2} \tag{1}$$

where, L is the length of the triangle base, c the velocity of light in free space, ε_r the relative dielectric coefficient of substrate, and integers m and n determine the resonant modes. When $m = 0$ and $n = 1$, the dominant mode is obtained, and its resonant frequency can be expressed as $f_{01} = \sqrt{2}c/(2L\sqrt{\varepsilon_r})$. Our research shows that the simulated results got by Ansoft ensemble [12] EM simulator based on method of moments (MoM) are similar to the calculation from Equation (1). Equation (1) is important for determining the resonant mode and helping design the required filter.

Table 1. TM modes for IRT patch resonator.

Mode sequence	m, n	$k_{m,n} \cdot \frac{L}{\pi}$	f_r
1	0, 1	$\sqrt{2}$	$f_{0,1} = \frac{\sqrt{2}}{2} \cdot \frac{c}{L\sqrt{\varepsilon_r}}$
2	1, 1	2	$f_{1,1} = \frac{c}{L\sqrt{\varepsilon_r}}$
3	1, -2	$\sqrt{7}$	$f_{1,-2} = \frac{\sqrt{7}}{2} \cdot \frac{c}{L\sqrt{\varepsilon_r}}$
4	2, 1	$2\sqrt{2}$	$f_{2,1} = \sqrt{2} \cdot \frac{c}{L\sqrt{\varepsilon_r}}$

Calculated TM mode properties of the IRT resonator are shown in Table 1. Calculated resonant performance variations of the IRT resonator are shown in Fig. 1, which shows resonant frequency decreases with triangle base L increasing. Fig. 2 shows the magnetic field patterns and current distributions of the IRT resonator with dual-mode operation. In this paper, all of the investigations are on IRT resonators and filters, and all of the calculations and designs are got by using ceramic substrate with dielectric constant of 10.2 and thickness of 1.27 mm.

3. RIGHT-ANGLED TRIANGULAR PATCH RESONATOR AND BANDPASS FILTER WITH REGULAR FRACTAL-SHAPED HOLE

We know that the basic fractal can be classified as Koch fractal, Minkowski fractal, Sierpinski fractal, and Hilbert fractal [13]. Classical Sierpinski fractal geometry is constructed by an isosceles triangle with a reversed isosceles triangle cut iteratively, and the cut parts have strict similarity in the whole structure, as shown in Fig. 3. In the research, we find that the strict Sierpinski fractal patch resonator is

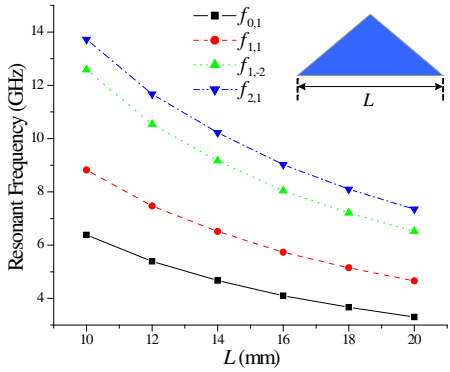

Figure 1. Simulated resonant frequency of the first four resonant modes for the IRT resonator.

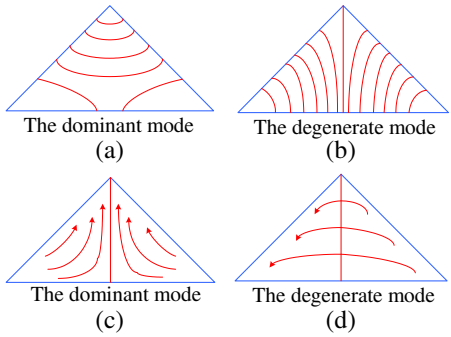

Figure 2. Magnetic field patterns and current distribution of the dominant and the degenerate modes for the IRT resonator, (a) and (b) are magnetic field patterns, (c) and (d) are current distribution.

hardly applied to a RF filter design because of the poor performance. In this part, all of the patch holes are right-angled triangle shape, i.e., fractal cut parts have strict similarity in the whole structure. However, it is not the Sierpinski fractal shape but a quasi one because the entire Sierpinski fractal for the IRT resonator cannot produce the desired filter performance.

Calculated resonant performance of the first two resonant modes for the right-angled triangular resonator with the 1st fractal is plotted in Fig. 4, and the calculations show that with the action of fractal, the resonant frequencies of the first two resonant modes are lower than those of the right-angled triangular resonator without patch hole, and a larger patch hole size introduces lower resonances. The calculated curves of parameters L versus l for the right-angeld

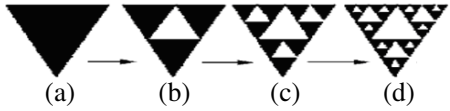

Figure 3. Sierpinski triangle iteration. (a) 0-th order. (b) 1st order. (c) 2nd order. (d) 3rd order.

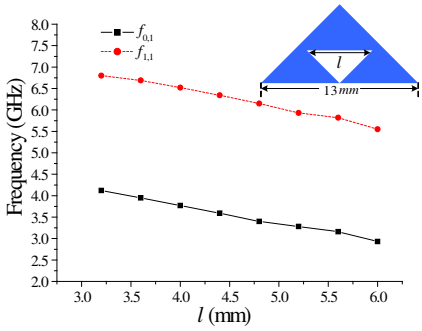

Figure 4. Resonant characteristics of the right-angled triangular resonator with the 1st fractal.

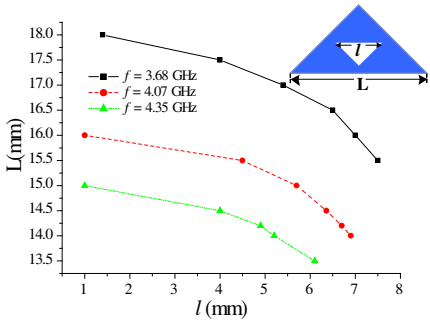

Figure 5. Calculated curves of parameter L versus l for the fractal right-angled triangular resonator at different resonances.

triangular resonator are plotted in Fig. 5, which shows that for a certain resonance, L decreases with increasing l, an advantage for miniaturization. Certainly, resonant frequency of the fractal IRT resonator increases with parameter L decreasing.

Transmission characteristic comparisons of the fractal right-angled triangular patch resonators are shown in Fig. 6, and all of the resonators are designed to have the same resonant frequency of 4.05 GHz. Figs. 6(a) and 6(b) plot the transmission characteristics of right-angled triangular resonator with the 1st and the 2nd order fractals, respectively, and both show that fractal resonator can be miniaturized when operating at the same resonant frequency. The two figures also show that for the fractal right-angled triangular patch resonator, a larger size of fractal hole introduces more miniature circuit dimension when operating at the same frequency, while resonant frequency band between the two higher order modes is extended. Transmission characteristic comparison of the right-angled triangular resonator with the 0-th, 1st and 2nd order fractals are shown in Fig. 6(c), which shows that the circuit size reduces with increasing fractal iteration order when operating at the same frequency. All these figures show that the dominant mode has the strongest resonance.

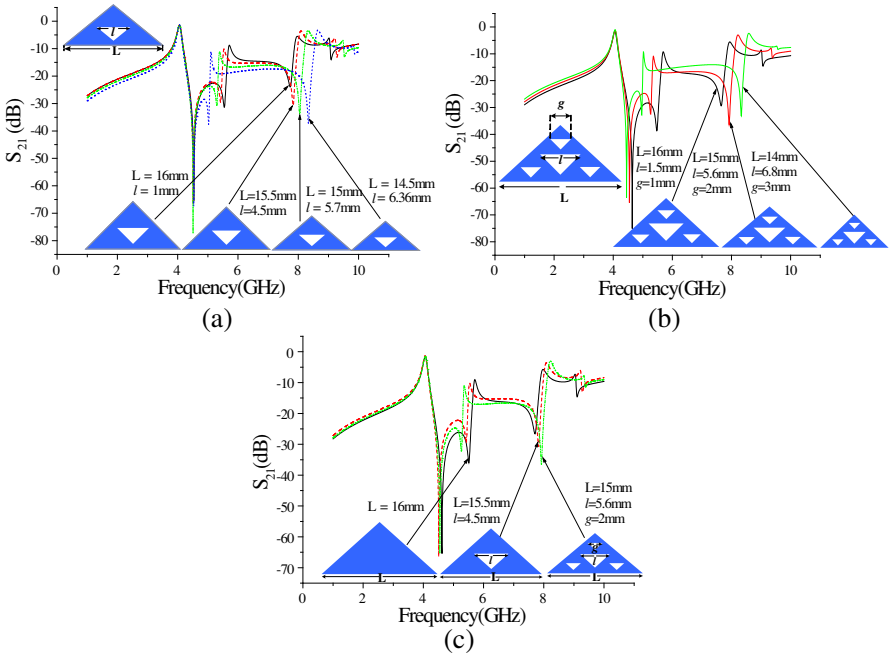

Figure 6. Transmission characteristics of the right-angled triangular resonator with the 0-th, the 1st and the 2nd fractal at 4.05 GHz. (a) Transmission characteristics of right-angled triangular resonator with the 1st fractal at 4.05 GHz. (b) Transmission characteristics of the right-angled triangular resonator with the 2nd fractal at 4.05 GHz. (c) Transmission characteristics of the right-angled triangular resonator with the 0-th, 1st and 2nd order fractal at 4.05 GHz.

The external quality factor of a single patch resonator may be expressed as $Q_{ei} = f_{0i}/\Delta f_{3\,\mathrm{dB}}$, where Q_{ei} is the external quality factor of the i-th resonant mode, and f_{0i} and $\Delta f_{3\,\mathrm{dB}}$ are the i-th resonant frequency and the corresponding 3-dB bandwidth of the single patch resonator, when the single patch resonator is externally excited alone. Calculated Q_e versus feeding position t of the right-angled triangular resonator with the 1st fractal is plotted in Fig. 7, which shows that the fractal resonator has adequate external quality factor of more than 127 and increases with increasing t.

Bandpass filters using single right-angled triangular patch resonator with the 1st and 2nd fractals are also designed, as shown in Fig. 8, where I/O feed lines set at the triangle bottom are microstrip lines with characteristic impedance of 50 Ω, and the fractal patterns are all right-angled triangular shapes which have strict similarity to

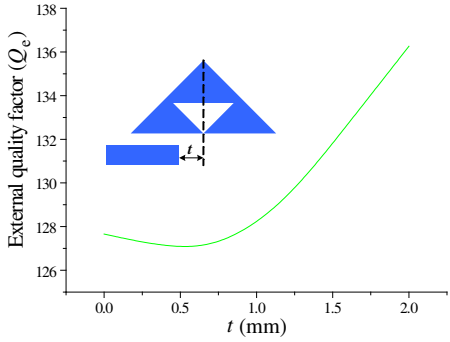

Figure 7. External quality factor Q_e versus feeding position t, $L = 13\,\text{mm}$, $l = 5\,\text{mm}$.

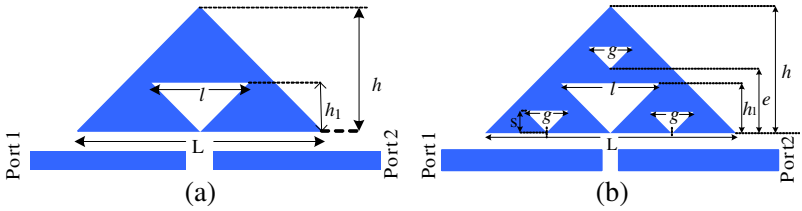

Figure 8. Topologies of the bandpass filter using single IRT patch resonator with fractal hole. (a) With the 1st fractal. (b) With the 2nd fractal.

the IRT patch resonator. Simulated frequency responses of the IRT resonator bandpass filter with the 1st fractal are shown in Fig. 9, which shows that filter performance is greatly improved with a better frequency selectivity and a wider bandwidth for the upper stopband, and filter operation frequency lowered from 5.0 GHz to 3.2 GHz with the assistance of a fractal pattern. These changes are due to fractal hole which brings perturbation to the original (the 0-th fractal) IRT resonator. The filter relative bandwidth and passband insertion loss are shown in Table 2.

In order to verify the design, the proposed filter as shown in Fig. 8(a) is fabricated, and the hardware and measurement are shown in Fig. 10. The circuit occupies an area of about $23 \times 8\,\text{mm}^2$. The measured results got by Agilent E5071C vector network analyser are close to the simulation, and the measured passband insertion loss at centre frequency is about 1.6 dB. Simulated frequency responses of the IRT resonator bandpass filter with the 2nd fractal as shown in Fig. 8(b) are plotted in Fig. 11, which shows that smaller fractal holes introduce increased operation frequency. The filter performance

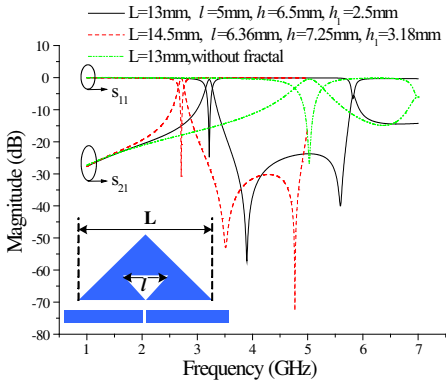

Figure 9. Simulated frequency responses of the IRT resonator bandpass filter with the 0-th and the 1st fractal.

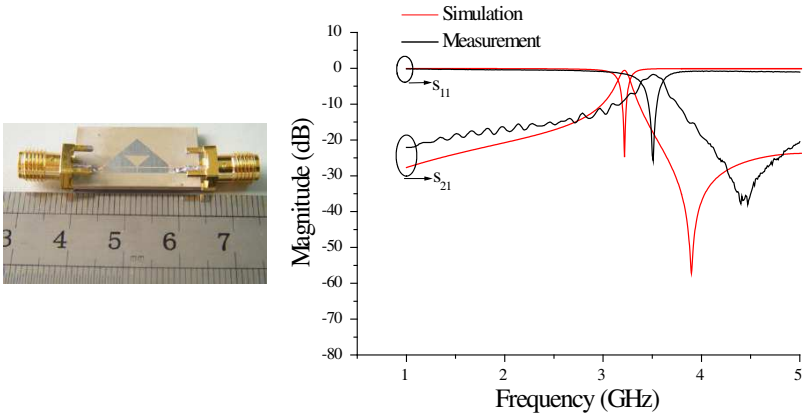

Figure 10. Filter fabrication and measurement, $L = 13\,\text{mm}$, $l = 5\,\text{mm}$. (a) Photograph of the fabricated hardware. (b) Comparison of the simulation and measurement.

is listed in Table 2. Fabricated hardware and measurement are shown in Fig. 12. It can be seen the measurement is similar to the simulation, and the measured passband insertion loss at the measured centre frequency of 2.98 GHz is about 1.2 dB. The circuit occupies an area of about $24 \times 8.4\,\text{mm}^2$. The filters with the 1st and 2nd fractals have similar performance, and both operate at the TM_{01} mode. For the two fabricated filters, the main error of the simulation and experiment is operation frequency shift, mainly due to the material discrepancy and fabrication uncertainty.

Table 2. simulated filter relative bandwidth and passband insertion loss (IL).

	Geometric parameters (mm)	Center frequency (GHz)	Relative bandwidth (%)	Passband IL (dB)
The 1st fractal	$L = 13$, $l = 5$	3.21	4.05	0.18
	$L = 14.5$, $l = 6.36$	2.69	4.09	0.12
The 2nd fractal	$L = 14$, $l = 6.8$	2.54	4.33	0.08
	$L = 14$, $l = 6$	2.80	3.2	0.15

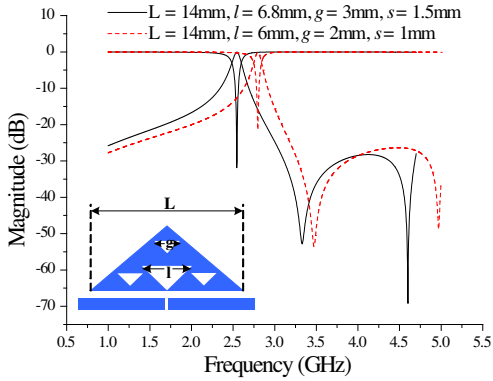

Figure 11. Simulated frequency responses of the IRT resonator bandpass filter with the 2nd fractal.

4. RIGHT-ANGLED TRIANGULAR PATCH RESONATOR WITH IRREGULAR FRACTAL-SHAPED HOLE

For IRT patch resonator with irregular fractal hole, calculated curves of resonant frequency versus parameter b, parameter h_1, and parameter d are shown in Fig. 13. It can be seen from Fig. 13(a) that the resonant frequencies of the first and second higher order modes decrease with parameter b increasing, while the dominant mode has nearly no variation. Fig. 13(b) shows that the variation of hole height h_1 has little effect on resonance of the higher order modes, but for the dominant mode, resonant frequency decreases with h_1 increasing, and it lowers much when the patch deleted triangle top approaches the IRT top.

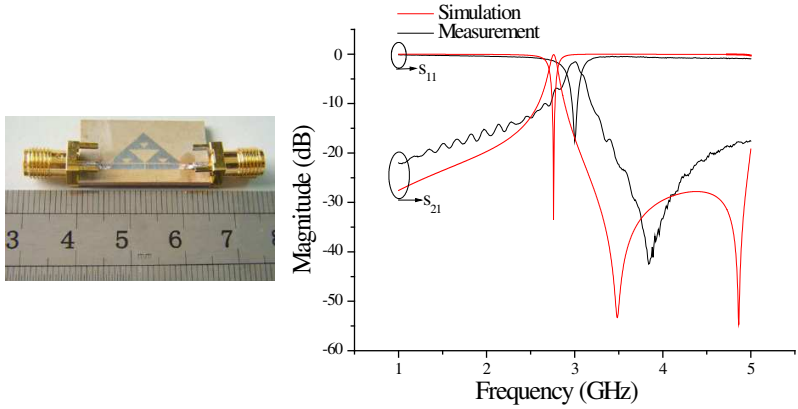

(a) (b)

Figure 12. Filter fabrication and measurement, $L = 14\,\text{mm}$, $l = 6\,\text{mm}$, $g = 2\,\text{mm}$, $s = 1\,\text{mm}$, $e = 3.5\,\text{mm}$, $h = 7\,\text{mm}$, $h_1 = 3\,\text{mm}$. (a) Photograph of the fabricated hardware. (b) Comparison of the simulation and measurement.

Parameter d has different effects on resonant modes, as shown in Fig. 13(c). It can be seen for the dominant mode, resonant frequency increases with increasing d when $d < 4\,\text{mm}$; however, the resonant frequency decreases abruptly when $d > 4\,\text{mm}$. For the first higher order mode, resonant frequency has no obvious change with parameter d, and for the second higher order mode, resonant frequency decreases with d increasing. It can be concluded that the higher order modes are mainly related with parameters b and d, and the dominant mode is mainly related with parameters h_1 and d. In the research, it is shown that the resonance of the first higher order mode may be suppressed when the triangle base b of fractal hole is big enough to cut the isosceles triangle side, and it is also shown that the fractal hole in IRT resonator described above is hard to make the dominant mode split to introduce a dual-mode filter and that the higher order modes, such as TM_{11}, $TM_{1,-2}$, are also hard to be splitted.

Transmission characteristics of the IRT resonator with irregular fractal hole are shown in Fig. 14. Figs. 14(a) and (b) show the transmission characteristics of the IRT resonator with single and double fractal holes which operate at 2.5 GHz and 2.4 GHz, respectively. Fig. 14(c) shows the transmission characteristics comparison of the IRT resonator without and with fractal holes which operate at 3.8 GHz. All of the figures illustrate that the resonator size reduction and spurious response improvements go together with the help of a fractal when the resonators operate at the same frequency.

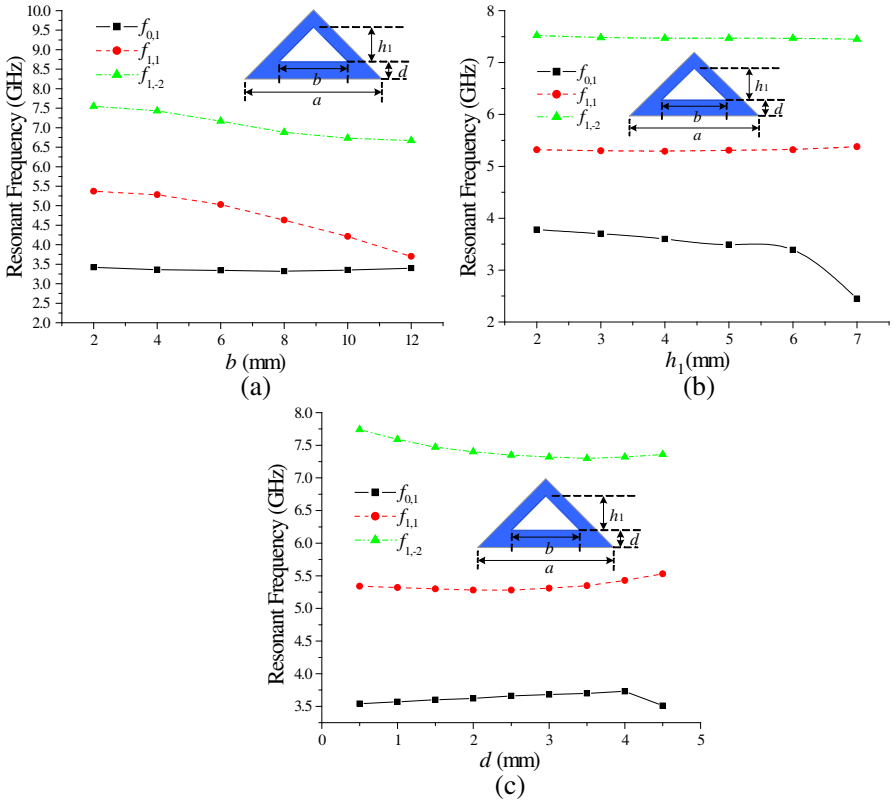

Figure 13. Calculated curves of the first three resonant frequencies versus geometric parameters for the IRT resonator with fractal hole. (a) Relationships of parameter b and resonant frequency, $a = 17\,\text{mm}$, $d = 1.5\,\text{mm}$, $h_1 = 6\,\text{mm}$. (b) Relationships of parameter h_1 and resonant frequency, $a = 17\,\text{mm}$, $b = 3.6\,\text{mm}$, $d = 1.5\,\text{mm}$. (c) Relationships of parameter d and resonant frequency, $a = 17\,\text{mm}$, $b = 3.6\,\text{mm}$, $h_1 = 5\,\text{mm}$.

5. RIGHT-ANGLED TRIANGULAR PATCH RESONATOR DUAL-BAND FILTER

Currently, many RF filters are designed with dual-band or multi-band operation because the increasing demand of wireless communication applications necessitates RF transceivers operating at dual-band or multi-band in order that users can access more services with a single handset. In this paper, single patch right-angled triangular resonator dual-band bandpass filters with irregular fractal patterns

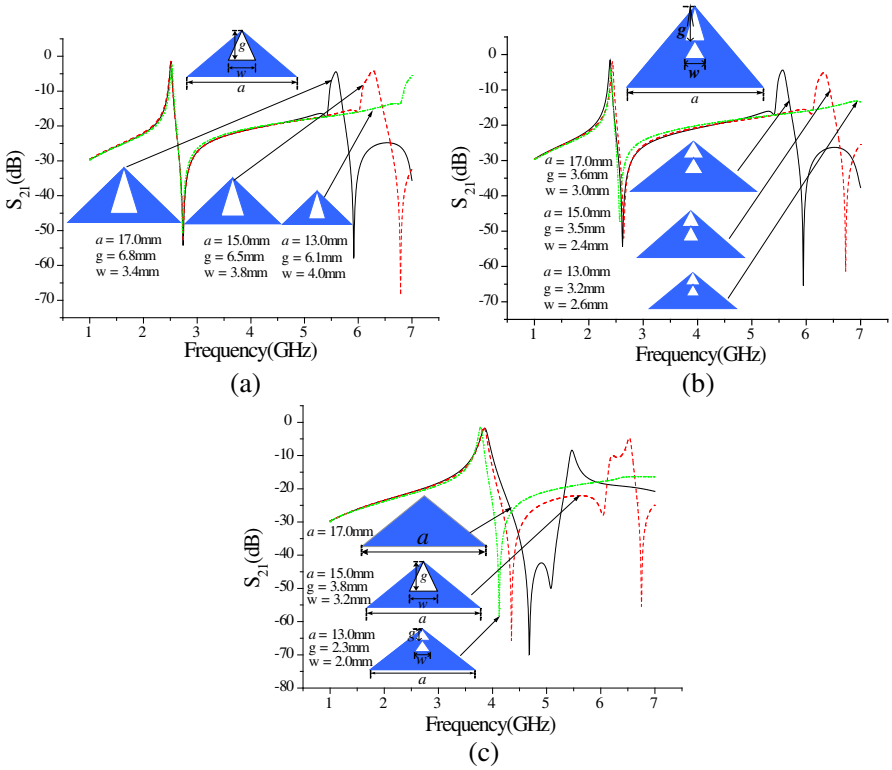

Figure 14. Transmission characteristics comparison of the IRT resonator with different fractal hole. (a) Transmission characteristics of the IRT resonator with single fractal hole at about 2.5 GHz. (b) Transmission characteristics of the IRT resonator with a pair of fractal holes at about 2.4 GHz. (c) Transmission characteristics of the IRT resonator without and with fractal hole at about 3.8 GHz.

are designed, as shown in Fig. 15, where the fractal hole which acts as perturbation is used to strengthen the required resonant modes, control the operation frequency, and suppress the undesired spurious responses. The operation dual-band is due to the application of the resonant modes, and the operation modes can be made certain by formula (1). The coupling structure and equivalent circuit plotted in Figs. 15(c) and (d) show that the operation of a IRT resonator with fractal hole is equivalent to the operation of resonator 1 denoted by a parallel circuit of L_1 and C_1, and resonator 2 denoted by a parallel circuit of L_2 and C_2 using two-path coupling. I/O feed lines denoted by capacitor C_4 are microstrip lines with characteristic impedance of 50 Ω,

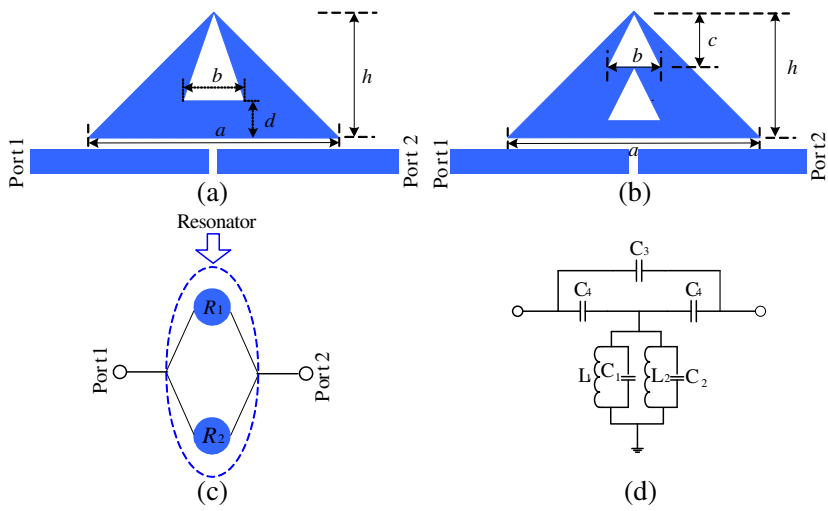

Figure 15. Dual-band bandpass filters using single IRT patch resonator with fractal hole, for topology 1, $a = 17\,\text{mm}$, $b = 3.6\,\text{mm}$, $d = 1.4\,\text{mm}$, $h = 8.5\,\text{mm}$; for topology 2, $a = 17\,\text{mm}$, $b = 3\,\text{mm}$, $c = 3.6\,\text{mm}$, $h = 8.5\,\text{mm}$. (a) Filter 1. (b) Filter 2. (c) Coupling structure. (d) Equivalent circuit.

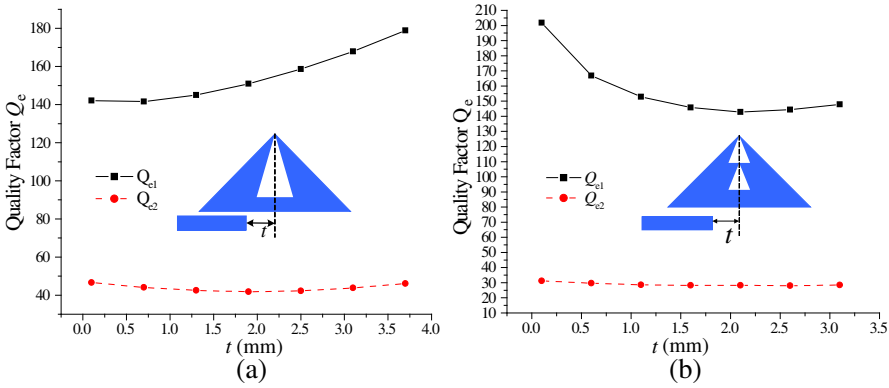

Figure 16. External quality factor Q_e versus feeding position t. (a) With a single hole. (b) With dual-hole.

and their coupling can be denoted by a capacitor C_3. The calculated external quality factor Q_e versus the feeding position t is plotted in Fig. 16, where Q_{e1} and Q_{e2} are external quality factors corresponding to the dominant mode and the first higher order mode, respectively. It

is shown that IRT resonator with a single and double fractal holes has adequate external quality factor.

Simulated frequency responses of filters 1 and 2 are shown in Fig. 17, and the corresponding performances are listed in Table 3. It is shown from calculation that the dual-band is got by resonances $f_{0,1}$ and $f_{1,1}$, respectively, and the filters have similar performances. Both of the dual-band filters operate at about 2.4 GHz and 5.5 GHz, respectively. It can be seen that if triangular patch hole has the same direction and similar area, the filters have similar frequency responses, and it also can be seen that with the assistance of fractal patterns, the resonant frequency of the dominant mode lowers, and the filter performance is greatly improved. In the research, we notice that the passband insertion loss of the second band for the single patch fractal

Table 3. simulated filter relative bandwidth and passband insertion loss (IL).

	The 1st passband		The 2nd passband	
	Relative bandwidth	Passband IL (dB)	Relative bandwidth	Passband IL (dB)
Filter 1	5.04%	0.27	2.0%	2.07
Filter 2	5.04%	0.3	1.8%	2.7
Filter 3	6.55%	0.18	3.2%	1.3
Filter 4	3.3%	0.4	3.9%	0.6
Filter 5	5.08%	0.25	3.38%	0.4

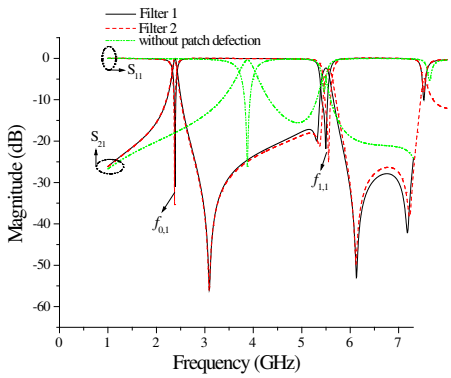

Figure 17. Simulated frequency responses of filter 1 and 2.

IRT filter is about 2 dB and improved to 1.3 dB when dual-patch (have the same size) fractal IRT resonators are applied, as shown in Fig. 18. Relative bandwidth and passband insertion loss of filter 3 are listed in Table 3.

In order to further enhance the passband insertion loss, dual-band bandpass filters with two-path coupling are developed, as shown in Fig. 19, and the filter coupling structure is plotted in Fig. 19(c), where R_i $(i = 1, 2)$ denotes the i-th resonator which introduces the i-th band. Here, for filter 4, $h_1 = 5.3\,\text{mm}$, $h_2 = 2.5\,\text{mm}$, $h_3 = 3.5\,\text{mm}$, $h_4 = 8\,\text{mm}$, $L_1 = 5\,\text{mm}$, $L_2 = 10.6\,\text{mm}$, $L_3 = 16\,\text{mm}$, $L_4 = 7\,\text{mm}$, and the patch holes are all isosceles right-angled triangle. For filter 5, $h_1 = 6.5\,\text{mm}$, $h_2 = 2.5\,\text{mm}$, $h_3 = 3.6\,\text{mm}$, $h_4 = 8.5\,\text{mm}$, $L_1 = 2\,\text{mm}$, $L_2 = 13\,\text{mm}$, $L_3 = 17\,\text{mm}$, $L_4 = 3\,\text{mm}$, and the patch holes are all isosceles triangles. Simulated filter frequency responses are shown in

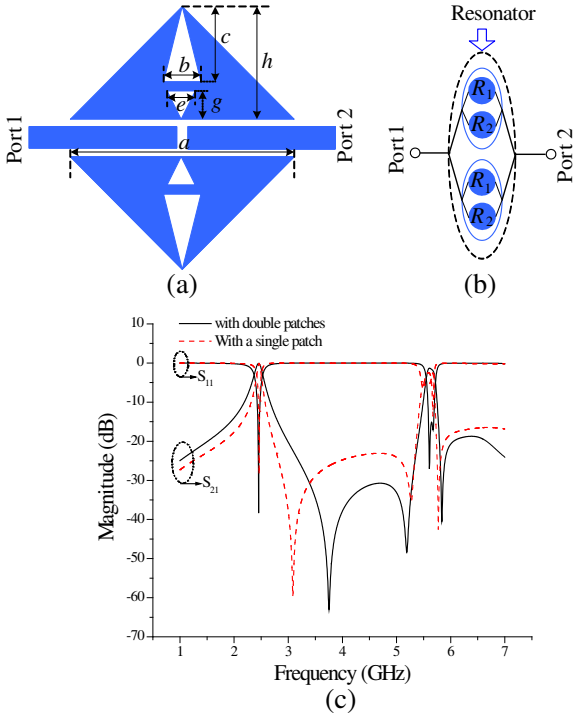

Figure 18. Dual-band bandpass filter using dual-patch IRT resonator with fractal holes, $a = 17\,\text{mm}$, $b = 3.2\,\text{mm}$, $c = 5.1\,\text{mm}$, $e = 2.8\,\text{mm}$, $h = 8.5\,\text{mm}$. (a) Filter 3. (b) Coupling structure. (c) Simulated filter frequency responses.

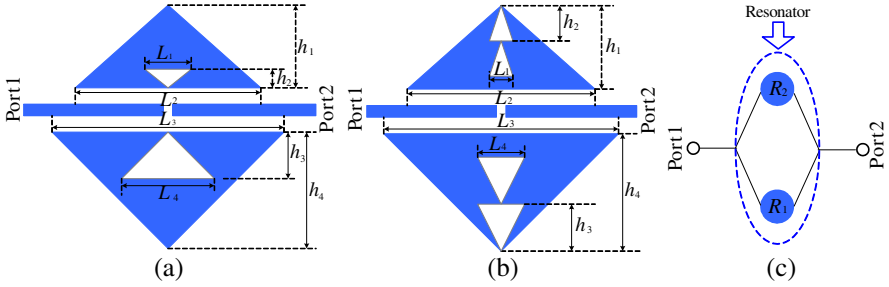

Figure 19. Dual-band bandpass filters using IRT patch resonators with fractal holes and two-path coupling. (a) Topology of filter 4. (b) Topology of filter 5. (c) Coupling structure.

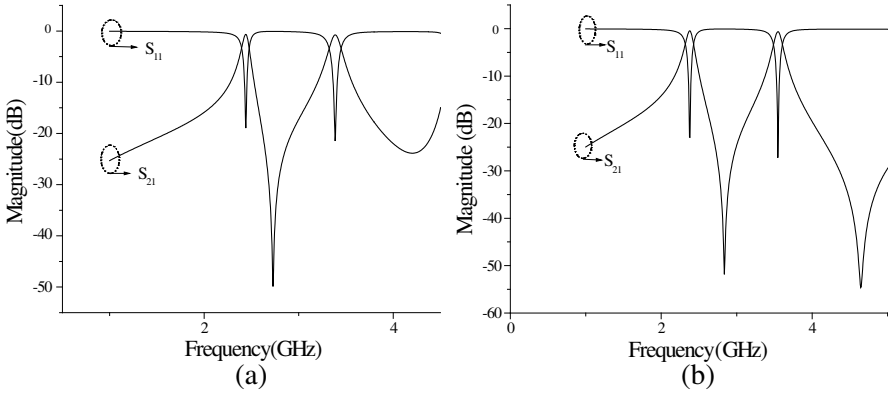

Figure 20. Simulated frequency responses of filter 4 and 5. (a) Frequency responses of filter 4. (b) Frequency responses of filter 5.

Fig. 20, and the filters performances are listed in Table 3. It can be seen that both filters 4 and 5 operate at about 2.4 GHz and 3.5 GHz with passband insertion loss of no more than 0.6 dB. Both filters 4 and 5 have circuit size of no more than $27 \times 17\,\text{mm}^2$.

The right-angled triangular resonator with fractal hole can also be used to design dual-band bandstop filter, as shown in Fig. 21, where $h_1 = 5.5\,\text{mm}$, $h_2 = 2\,\text{mm}$, $h_3 = 3\,\text{mm}$, $h_4 = 7.5\,\text{mm}$, $L_1 = 1.5\,\text{mm}$, $L_2 = 11\,\text{mm}$, $L_3 = 15\,\text{mm}$, $L_4 = 2\,\text{mm}$, and the coupling structure is the same as in Fig. 19(c). Simulated frequency responses are plotted in Fig. 21(b), and it can be seen that the dual-band bandstop filter operates at about 3.06 GHz and 4.53 GHz with relative bandwidths of 2.6% and 2%, respectively.

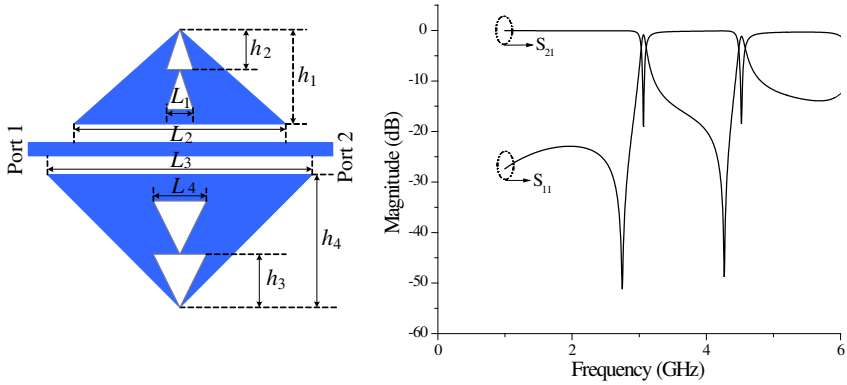

Figure 21. Dual-band bandstop filter using IRT patch resonators with fractal holes and two-path coupling. (a) Filter topology. (b) Simulated frequency responses.

6. CONCLUSION

Fractal-shaped isosceles right-angled triangular patch resonators are analyzed, and new RF filters have been developed. The filter design is demonstrated by experiment. It is shown that the IRT resonator and filter can be miniaturized with the assistance of a fractal, and the fractal enables the implementation of dual-band filters. The analysis and design method for the IRT resonator also can be applied to the equilateral triangular resonator and even the other patch resonators. The proposed right-angled triangular patch filters have good filter performances and compact, simple and miniature structures which are easy for fabrication. The dual-band bandpass filters meet IEEE 802.11 application requirements.

ACKNOWLEDGMENT

This work was supported in part by the Research Fund of China State Key Laboratory of Millimeter Waves (K201107) and Fundamental Research Funds for China Central Universities.

REFERENCES

1. Hong, J. S. and S. Li, "Theory and experiment of dual-mode microstrip triangular-patch resonators and filters," *IEEE Trans. on Microwave Theory and Techniques*, Vol. 52, 1237–1243, 2004.

2. Xiao, J.-K., Q.-X. Chu, and S. Zhang, "Novel microstrip triangular resonator bandpass filter with transmission zeros and wide bands using fractal-shaped defection," *Progress In Electromagnetics Research*, Vol. 77, 343–356, 2007.
3. Hong, J. S., "Microstrip dual-mode band reject filter," *IEEE MTT-S International Microwave Symposium Digest*, 945–948, 2005.
4. Helszajn, J. and D. S. James, "Planar triangular resonators with magnetic walls," *IEEE Trans. on Microwave Theory and Techniques*, Vol. 26, 95–100, 1978.
5. Alhawari, A. R. H. and A. Ismail, "Compact wideband bandpass filter using single corners-cut isosceles triangular patch resonator," *Progress In Electromagnetics Research C*, Vol. 14, 227–237, 2010.
6. Xiao, J.-K., "Triangular resonator bandpass filter with tunable operation," *Progress In Electromagnetics Research Letters*, Vol. 2, 167–176, 2008.
7. Kim, I. K., N. Kingsley, M. Morton, et al., "Fractal-shaped microstrip coupled-line bandpass filters for suppression of second harmonic," *IEEE Trans. on Microwave Theory and Techniques*, Vol. 53, 2943–2948, 2005.
8. Yousefzadeh, N., C. Ghobadi, and M. Kamyab, "Consideration of mutual coupling in a microstrip patch array using fractal elements," *Progress In Electromagnetics Research*, Vol. 66, 41–49, 2006.
9. Asad, H., M. Zubair, and M. J. Mughal, "Reflection and transmission at dielectric-fractal interface," *Progress In Electromagnetics Research*, Vol. 125, 543–558, 2012.
10. Li, T., G.-M. Wang, K. Lu, et al., "Novel bandpass filter based on CSRR using koch fractal curve," *Progress In Electromagnetics Research Letters*, Vol. 28, 121–128, 2012.
11. Bahl, I. and P. Bhartia, *Microwave Solid State Circuit Design*, John Wiley & Sons Press, New York, 1988.
12. Ansoft Ensemble 8.0, Ansoft Inc..
13. Jarry, P. and J. Beneat, *Design and Realization of Miniaturized Fractal RF and Microwave Filters*, John Wiley & Sons Press, New York, 2009.